



Calhoun: The NPS Institutional Archive
DSpace Repository

Theses and Dissertations

1. Thesis and Dissertation Collection, all items

1960

Some examples of exponential refractivity distributions.

Waldron, Charles G.

Monterey, California. Naval Postgraduate School

<http://hdl.handle.net/10945/13064>

Downloaded from NPS Archive: Calhoun



Calhoun is the Naval Postgraduate School's public access digital repository for research materials and institutional publications created by the NPS community. Calhoun is named for Professor of Mathematics Guy K. Calhoun, NPS's first appointed -- and published -- scholarly author.

Dudley Knox Library / Naval Postgraduate School
411 Dyer Road / 1 University Circle
Monterey, California USA 93943

<http://www.nps.edu/library>

NPS ARCHIVE
1960
WALDRON, C.

SOME EXAMPLES OF EXPONENTIAL
REFRACTIVITY DISTRIBUTIONS

CHARLES G. WALDRON

Thesis
W2203

Library
U. S. Naval Postgraduate School
Monterey, California

SOME EXAMPLES OF
EXPONENTIAL REFRACTIVITY DISTRIBUTIONS

by

Charles G. Waldron

//

Lieutenant, United States Naval Reserve

Submitted in partial fulfillment of
the requirements for the degree of

MASTER OF SCIENCE
IN
METEOROLOGY

United States Naval Postgraduate School
Monterey, California

1 9 6 0

NPS Archive
1960
Waldron, C.

~~W 203~~

SOME EXAMPLES OF
EXPONENTIAL REFRACTIVITY DISTRIBUTIONS

by

Charles G. Waldron

This work is accepted as fulfilling
the thesis requirements for the degree of

MASTER OF SCIENCE

IN

METEOROLOGY

from the

United States Naval Postgraduate School

ABSTRACT

Recently, exponential models of refractivity have been devised by several investigators to replace the linear, "standard" refractive atmosphere. In this study, average values of N are evaluated from the data at the mandatory radiosonde levels up to 25 mb, and mean coefficients c_i satisfying $N_{i+1} = N_i e^{-c_i(z_{i+1} - z_i)}$ have been evaluated for a group of eight mid-latitude stations, and for the entire winter season of 1958-59. The coefficients c_i , plotted as functions of the height of the i -th layer-center, possess certain characteristic features in common at all stations.

The writer wishes to express his appreciation for the assistance and encouragement given him by Professor Frank L. Martin of the U. S. Naval Postgraduate School in this investigation.

TABLE OF CONTENTS

Section	Title	Page
1.	Introduction	1
2.	Data-processing	3
3.	Discussion and Results	
	(a) Typical Model	7
	(b) Adak	9
	(c) Denver	10
	(d) Ship "P", Tatoosh Island, Kodiak, Washington, D. C.	11
	(e) Ship "N"	11
	(f) Lake Charles	20
	(g) Composite	20
4.	Other Applications	21
5.	Bibliography	24

LIST OF ILLUSTRATIONS

Figure	Page
1. Schematic model	8
2. Graph of c_i vs height for Adak	10
3. Graph of c_i vs height for Denver	12
4. Graph of c_i vs height for Ship P	13
5. Graph of c_i vs height for Tatoosh Island	14
6. Graph of c_i vs height for Kodiak	15
7. Graph of c_i vs height for Washington, D. C.	16
8. Graph of c_i vs height for Ship N	17
9. Graph of c_i vs height for Lake Charles	18
10. Graph of c_i vs height composite for all stations	19

LIST OF TABLES

Table	Page
1. Three month mean-values of N_i at indicated pressure levels, and stations employed in this study (in N - units)	6

LIST OF SYMBOLS USED

n = Index of refraction

N = Refractivity

T = Temperature in degrees Kelvin

p = Pressure in millibars

e = vapor pressure in millibars

z = Height in meters

δ_A = Autoconvective lapse rate

δ = Atmospheric lapse rate

K = Curvature of a ray

β = Ray-direction relative to the spherically horizontal level

a = Radius of the earth

\bar{c} = Empirical constant, affording best fit of an exponential formula

c_i = Mean value of c satisfying $N_{i+1} = N_i e^{-c_i (Z_{i+1} - Z_i)}$
where $Z_{i+1} - Z_i$ is the thickness of the i -th standard layer

1. Introduction

The refractive index n is defined as the ratio of the speed of an electromagnetic wave in a vacuum to the wave speed in the medium concerned. However, this particular form of the refractive index is not very convenient in the computation of ray-paths; hence the modified refractive index, N is normally used.

The refractivity N , which is equal to $(n-1) \times 10^6$, may be obtained from radiosonde observations using the equation

$$N = \frac{A}{T} \left(p + \frac{B e}{T} \right) = (n-1) \times 10^6 \quad (1)$$

where T is the temperature in degrees Kelvin, p is the pressure in millibars, e is the vapor pressure in mbs, and A and B are constants.

Using the Smith & Weintraub [4] values of these constants, Equation (1) may be written:

$$N = \frac{77.6 P}{T} + \frac{373256 e}{T^2} \quad (2)$$

A "standard" distribution of N in the vertical may be obtained by averaging over a sufficient number of individual soundings. Bean and Thayer [1] have suggested that its curve can be fitted by an exponential formula. The model which has recently been adopted by the National Bureau of Standards is of form:

$$N = N_s e^{-\bar{c} z} \quad (3)$$

where N is the refractive index at any altitude,

N_s is the mean surface value of the refractive index,

z is the height above the surface,

\bar{c} is an empirical constant, affording "best fit" in Equation (3).

Equation (3) is used only with the mean values of N averaged over a long enough period to eliminate all transitory trapping layers. The study by Bean and Thayer [1] also suggested further study by obtaining individual values of N_s and \bar{c} for varying climatic regions. This was the objective of the first approach of this author to the problem. Later, however, it was decided to make a finer-scale determination of the parameter \bar{c} by determining a mean-value c_i for each layer between mandatory levels. Thus a working equation of form

$$N(z) = N_i e^{-c_i(z-z_i)}, \quad z_i \leq z \leq z_{i+1} \quad (4)$$

was employed. Here c_i is temporarily assumed to be constant in the i -th layer, which extends from z_i to z_{i+1} and N_i is the value of N at $z = z_i$. Note finally that c_i may be obtained by differentiation of (4) as

$$C_i = -\frac{1}{N} \frac{dN}{dz} \quad (5)$$

2. Data Processing

The stations utilized in this study were selected to represent a wide variety of climatic regions. The c_i -values were determined from the three-month means of pressure, temperature, and moisture content, for all the mandatory levels at these stations during the winter of 1958-59. These data were obtained from the radiosonde checked data found in the Northern Hemisphere Data Tabulations Daily Bulletins [2] .

The use of data obtained from radiosondes introduced some uncertainty of the relative humidity when "motorboating" was reported. However, motorboating usually occurred near 400 mb, and there the error introduced by omitting "motorboating" reports from the moisture-averaging process was found to be ≤ 0.1 mb. The twice-daily observations taken at 0000 and 1200 Greenwich times were averaged. This served to filter out the diurnal variation, and to make the stations, some of which were separated by as much as six hours time-difference, more compatible. Two methods were used in obtaining the values utilized for the determination of the surface refractive index data. When the surface report was part of the published radiosonde, this was the preferred data-source. When this radiosonde level was not available, it was necessary to employ the surface observation for the station. However the surface observation was recorded only once each day, at 1200Z, and this would result in a comparison of a once-daily observation

against a twice daily one when going from the surface to 850 millibars. As a test, the surface three-month mean N-value for Washington was computed using both methods and a difference of only one N-unit in 300 was noted. Since Washington had one of the largest surface diurnal variations of the stations studied, this indicated that the once-a-day surface observation reports could be substituted for the two-a-day radiosonde surface reports without serious error.

For the actual determination of mean values, the standard levels from the surface up to 25 mbs were used. The twice-daily observations at these levels were totaled and then divided by the total number of entries. All the calculations were done on either tape adding machines or hand calculators. A maximum of 180 observations were used for each level, provided that no data were missing. The mean vapor pressure was obtained by determining the vapor pressure from each observation using the temperature and relative humidity data, and finding the mean of these. For the majority of the stations, moisture was recorded only up to the 400-mb level, at which level the vapor pressure was found to be less than 1 mb. The only station that had moisture data for the 300-mb level showed the mean vapor pressure to be less than one-tenth of a mb. This showed that very little accuracy would be lost by not including moisture considerations above 400 mbs.

After the three-month mean values of pressure, temperature, and vapor pressure were obtained for the mandatory levels of each station, the three-month mean N_i values were determined

for these levels using Equation (2). These values and the appropriate pressure levels are given in Table 1.

The c_i -values for each layer were obtained using the refractivity equation in the form:

$$c_i = - \frac{\ln \frac{N_{i+1}}{N_i}}{z_{i+1} - z_i} \quad (6)$$

where $z_{i+1} - z_i$ is the average-value of the thickness in the standard layers employed in this study.

The values of c_i for each station were then plotted on two cycle semi-logarithmic paper versus the midpoint-height of each layer as ordinate. These midpoints were taken from the U. S. Standard Atmosphere elevations for the stated pressure. A discussion of these results and of some applications are given in the following sections.

$\frac{P}{N_1}$ Pressure	Adak 3 Meters*	Denver 1611 Meters	Ship P 6 Meters	Tatoosh 31 Meters	Kodiak 8 Meters	Washington 88 Meters	Ship N 6 Meters	Lake Charles 5 Meters
Surface	313 (1003.1mb)	254 (831.7mb)	314 (992.6mb)	323 (1014.8mb)	311 (1002.8mb)	310 (1009.7mb)	328 (1021.mb)	345 (1020.0mb)
850	262	---	261	266	262	261	268	272
700	216	212	214	217	217	217	217	216
500	161	157	158	159	161	158	156	154
400	134	131	131	131	133	130	128	128
300	105	103	103	104	105	102	100	101
250	100	88	87	89	88	88	87	87
200	71	72	70	71	70	71	72	71
150	52	54	52	53	52	54	55	55
100	35	36	35	36	35	36	38	38
50	17	18	17	18	17	18	19	18
25	9	9		9	9	9	9	9

* Surface height is listed under each station; station pressure is enclosed in parentheses.

Table 1. Three month mean-values of N_1 at indicated pressure levels, and stations employed in this study (in N-units):

3. Discussion and Results

(a) Typical Model

By Equation (5), c_i is a good indication of the vertical distribution of N . An increasing value of c_i indicates a larger rate of decrease of N with height. Most stations studied showed two main values of c_i in the vertical. A nearly constant value was indicated for the troposphere, and a somewhat larger value shown for the stratosphere. These values were separated at most stations by a characteristic feature, which will be referred to as a dual discontinuity. The dual discontinuity is evidently associated with the tropopause; it can be described as having a minimum value of c_i and immediately above it a pronounced increase to a maximum value. A model of c_i vs height which depicts schematically the association between the dual discontinuity and the related temperature sounding is shown in Figure 1, which may be regarded as typical of most mid-latitude stations.

In order to understand the association depicted in Figure 1, consider N as given by Equation (2) with $e=0$. Then

$$N = 77.6 \left(\frac{P}{T} \right) \quad (7)$$

Partial differentiation of N in (7) with respect to z , and use of the hydrostatic equation, leads to

$$\frac{\partial N}{\partial z} = - \frac{77.6}{T^2} P (\gamma_A - \gamma)$$

where γ_A is the autoconvective lapse rate, and γ is the

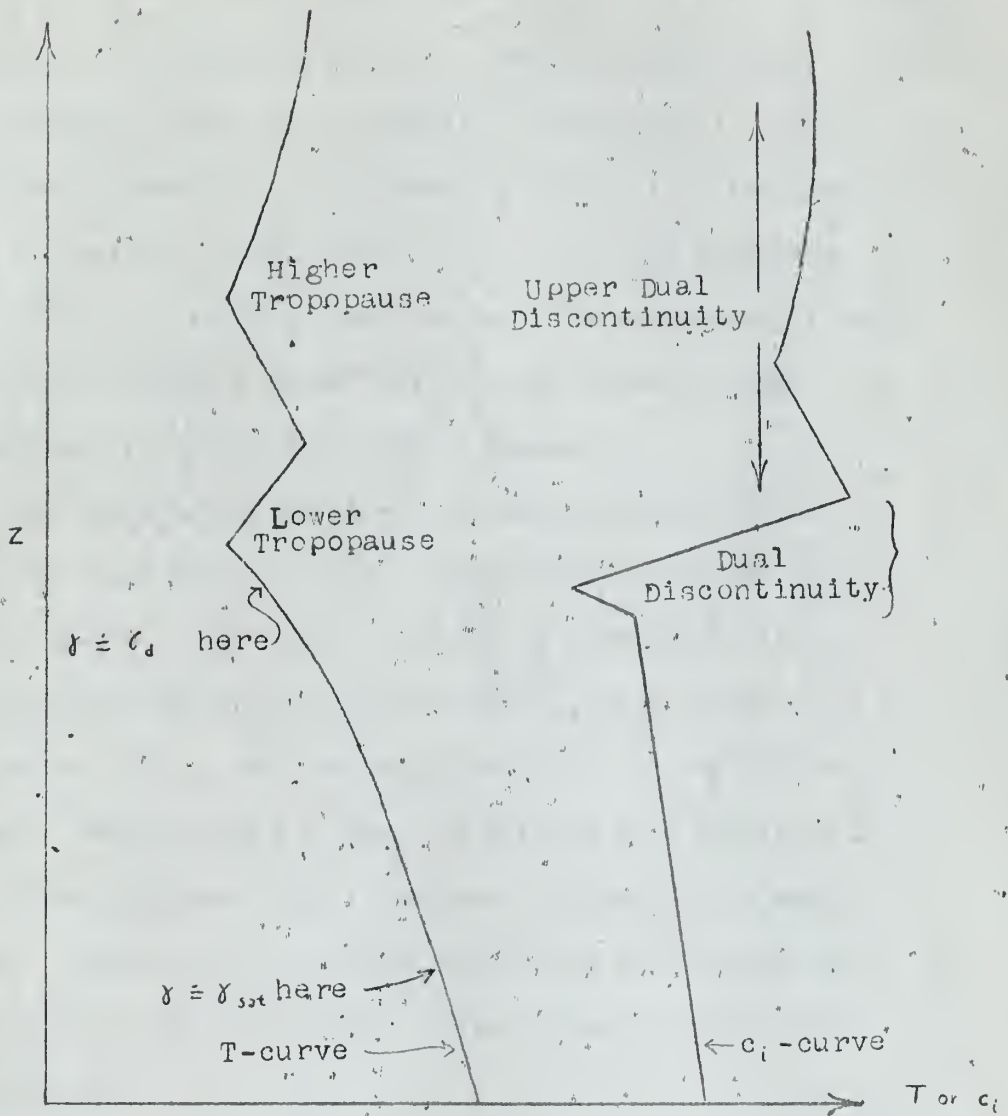


Figure 1, Schematic relationship between the radiosonde and the associated refractivity profile, for mid-latitude stations.

atmospheric lapse rate. By use of Equation (5), it follows that

$$c_i = \frac{1}{T} (\gamma_A - \gamma) \quad (8)$$

Hence c_i is relatively large in a thermally stable layer and relatively small in a thermally unstable layer. Thus if we disregard moisture, any minimum value of c_i is associated with a relatively steep lapse in the layer, and a maximum value with a relatively stable lapse. The discussion of the individual stations, which follows, will point out some deviations from the typical model, Figure 1.

One can also qualitatively estimate what the effect of moisture lapse would be on c_i . Empirically one knows that a large negative value of dN/dZ may be associated with a strong hydrolapse and this would cause c_i to be large [Equation (5)]. On the other hand, if the temperature lapse is not abnormal, c_i may be a minimum as a result of a small lapse (or possibly an increase with height) of water vapor. Moisture effects may be associated with some of the deviations of the individual c_i graphs from the ideal one of Figure 1.

(b) Adak

The tropospheric distribution of c_i vs height, Figure 2, showed a gradual decrease of c_i with increasing height up to 9 km. Above this level, a pronounced dual discontinuity was found, indicating the presence of a tropopause

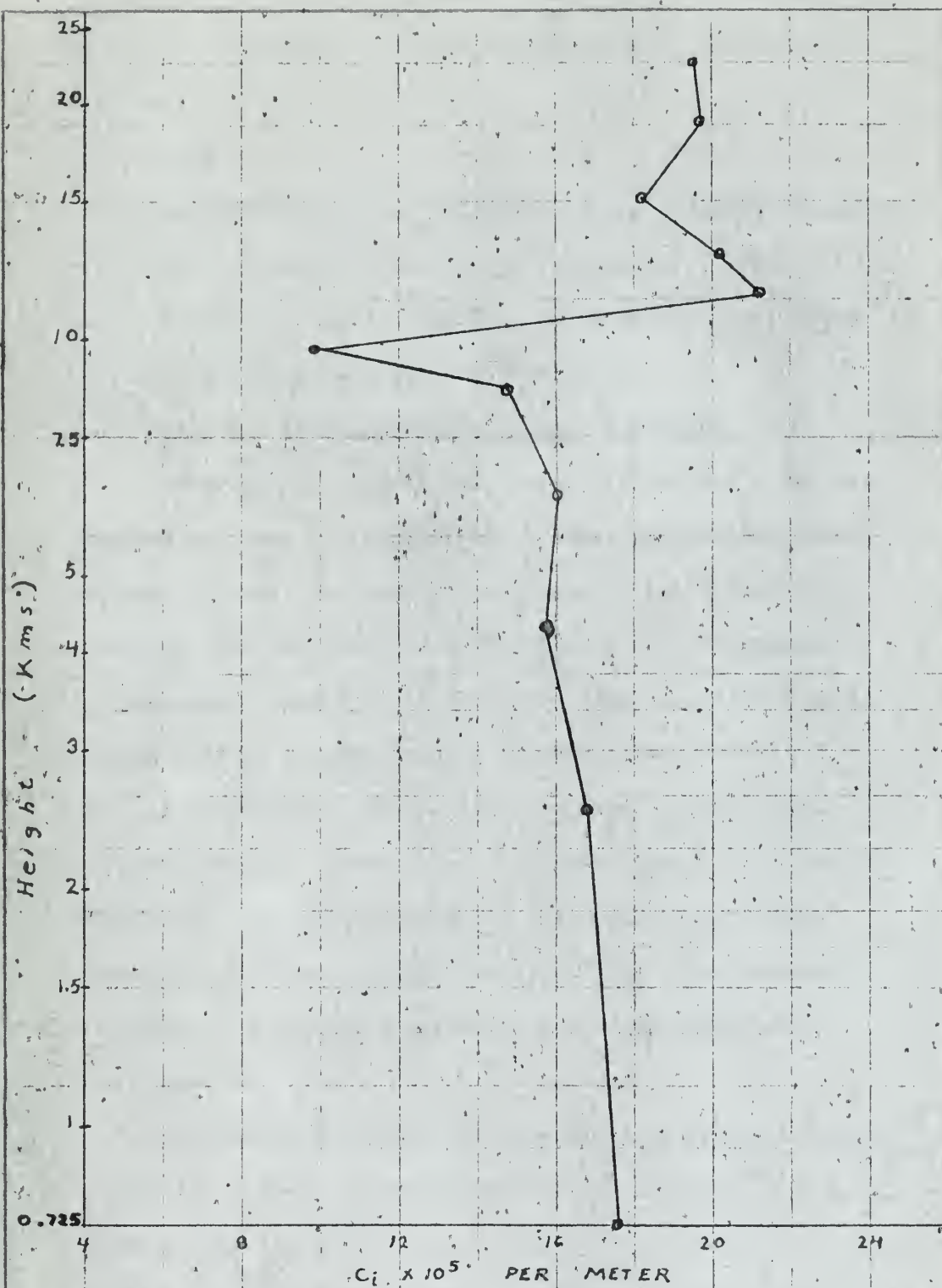


Figure 2. The graph of C_1 vs height for Adak.

layer. A second dual discontinuity of lesser magnitude was noted above the first. This was taken as an indication of a multiple tropopause, which is in keeping with the model of Figure 1.

(c) Denver

The graph for Denver, Figure 3, shows a smaller value of c_i in the troposphere than in the stratosphere. There is a sharp increase in c_i to a maximum value near 13 km, with no definite dual-discontinuity minimum below.

(d) Ship "P", Tatoosh Island, Kodiak, Washington, D.C.

The graphical results for these stations are shown in Figures 4, 5, 6, 7, respectively. These graphs have been grouped together because they all have features closely resembling the idealized model of Figure 1. The tropospheric c_i decreases slightly with elevation, and is followed by a faster rate of decrease ending in the region of 8-10 km. The stratospheric c_i then conforms rather closely to the schematic model. Kodiak shows a lesser tendency to have the pronounced minimum c_i as part of its dual discontinuity. This might well be a characteristic of its higher latitude, together with a greater variability of tropopause height.

(e) Ship "N"

The graphical results for this station, Figure 8, shows a greater decrease of tropospheric c_i with elevation than is shown in the idealized model. This is due primarily to the greater moisture content, and consequently greater N-value, in

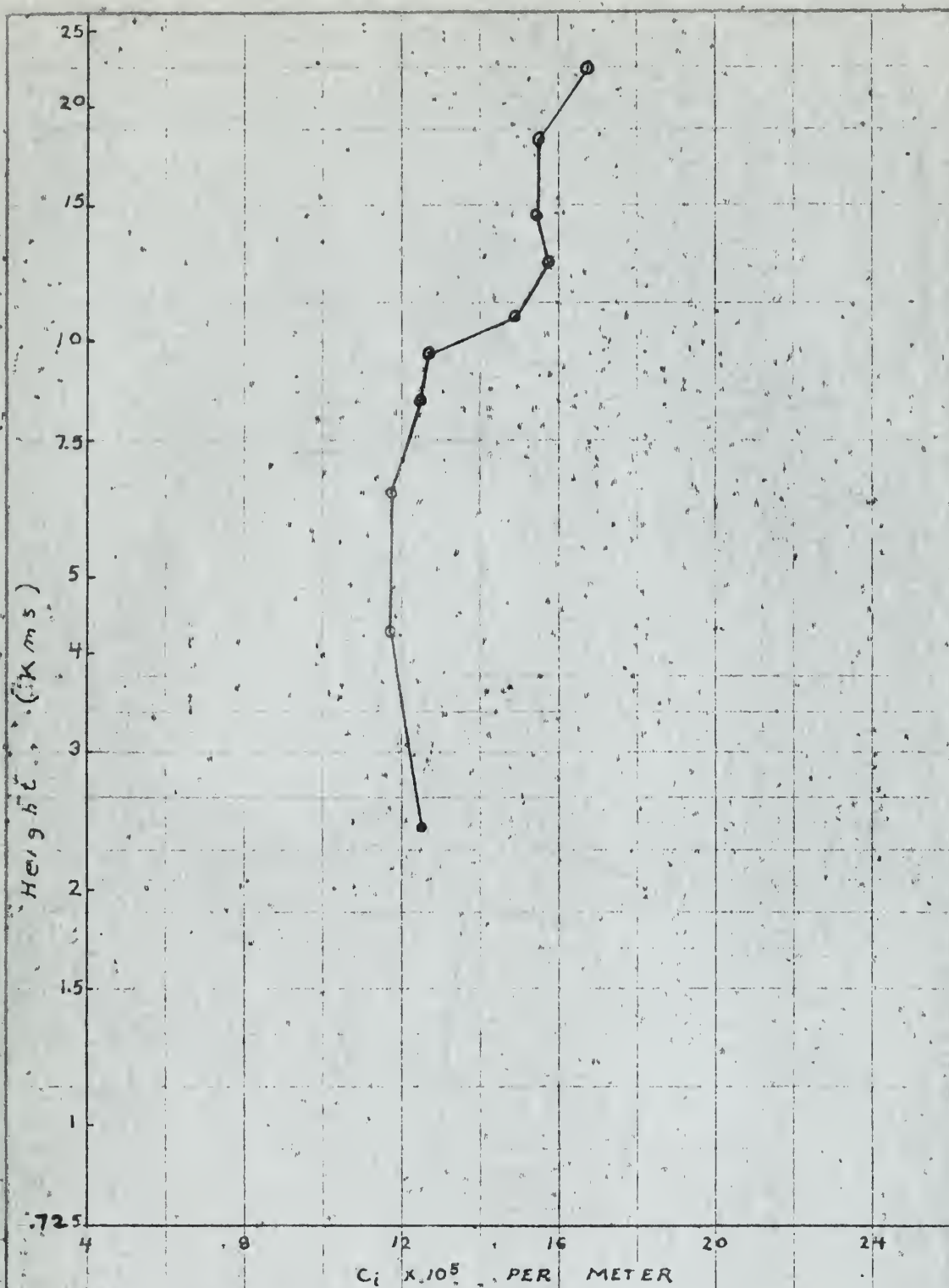


Figure 3. The graph of C_i vs. height for Denver.

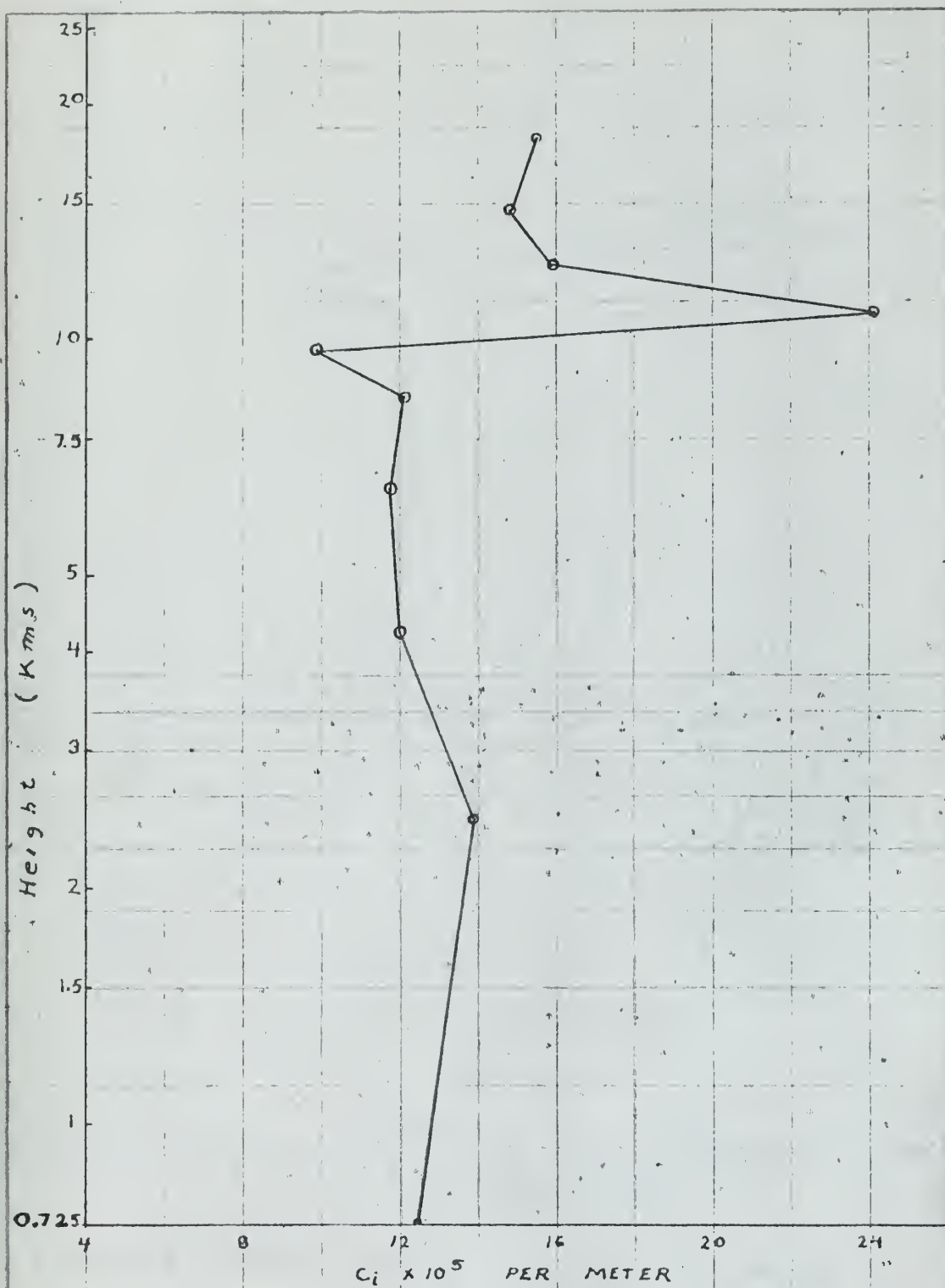


Figure 4 The graph of C_i vs height for Ship "P"

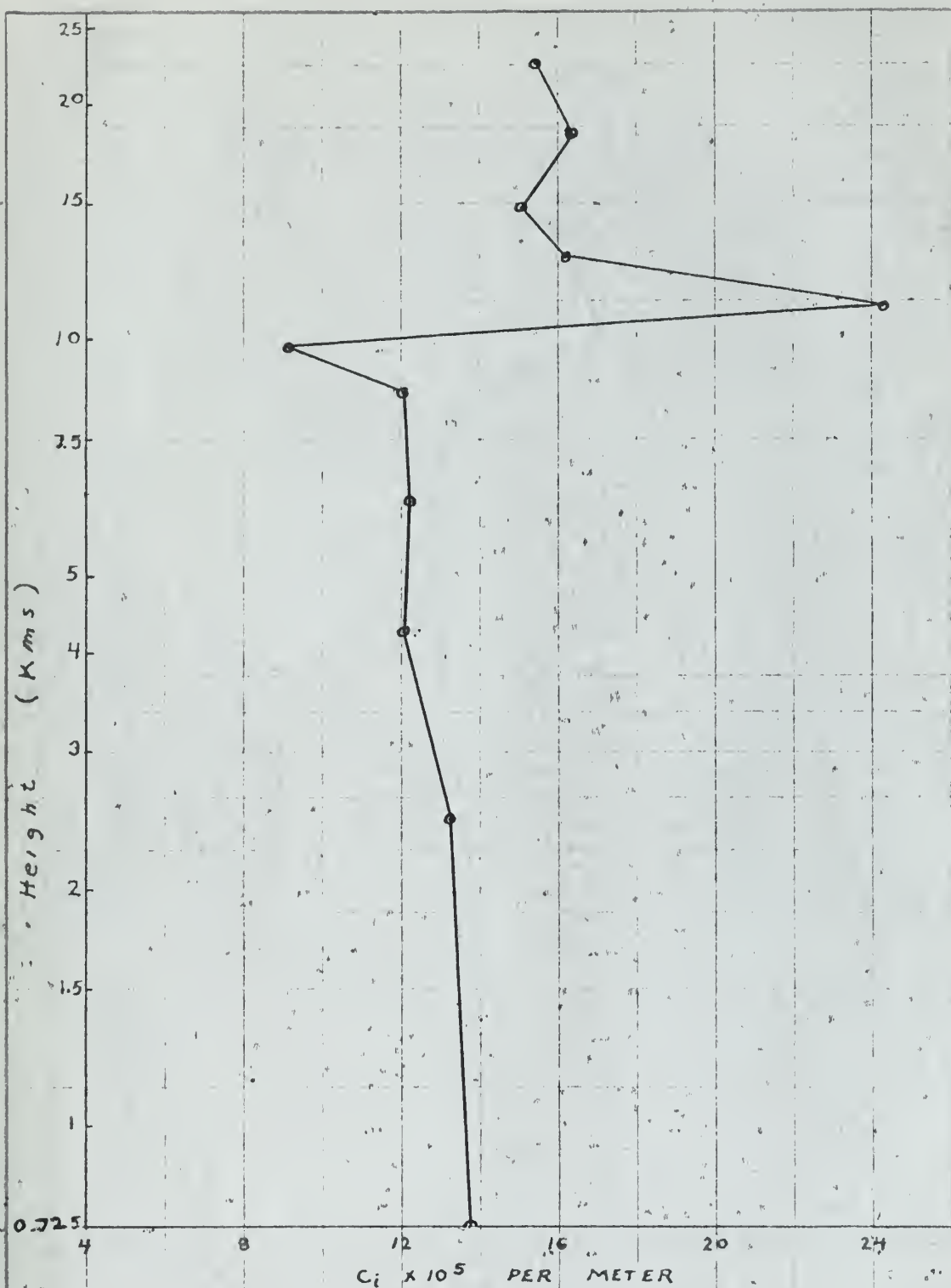


Figure 5. The graph of C_i vs height
for Tatoosh Island

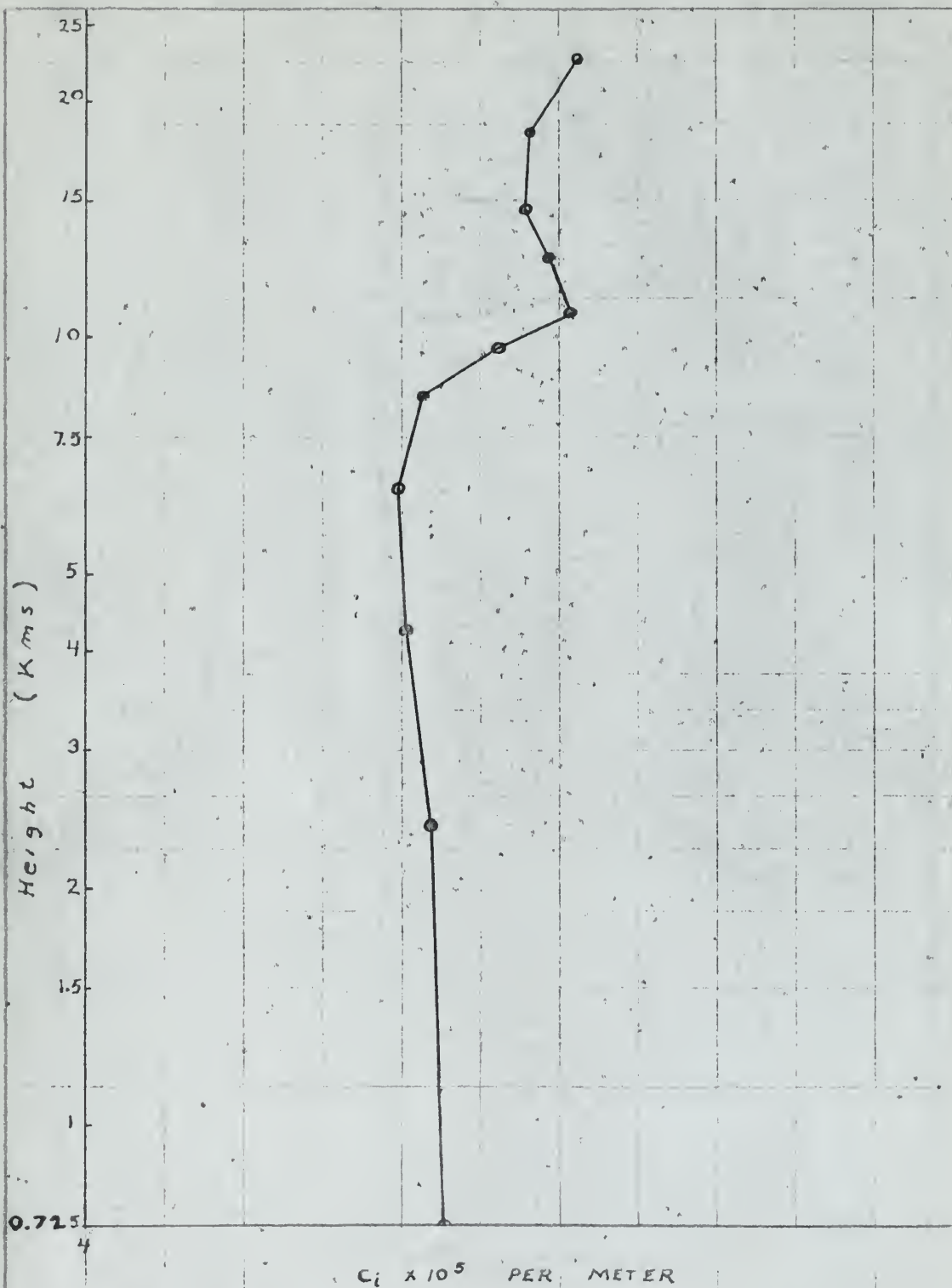


Figure 6. The graph of C_i vs height
for Kodiak

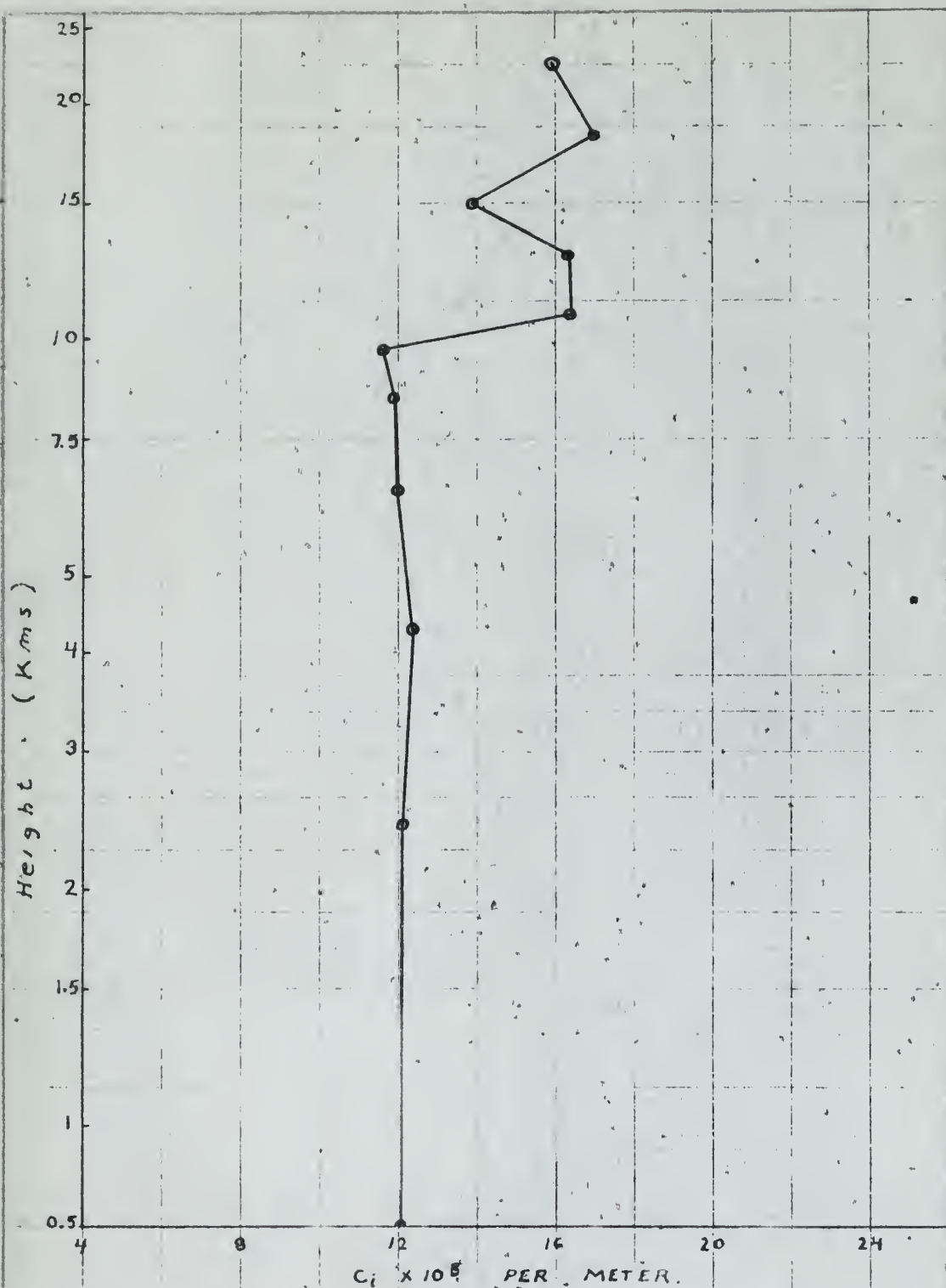


Figure 7. The graph of C_i vs height for Washington, D.C.

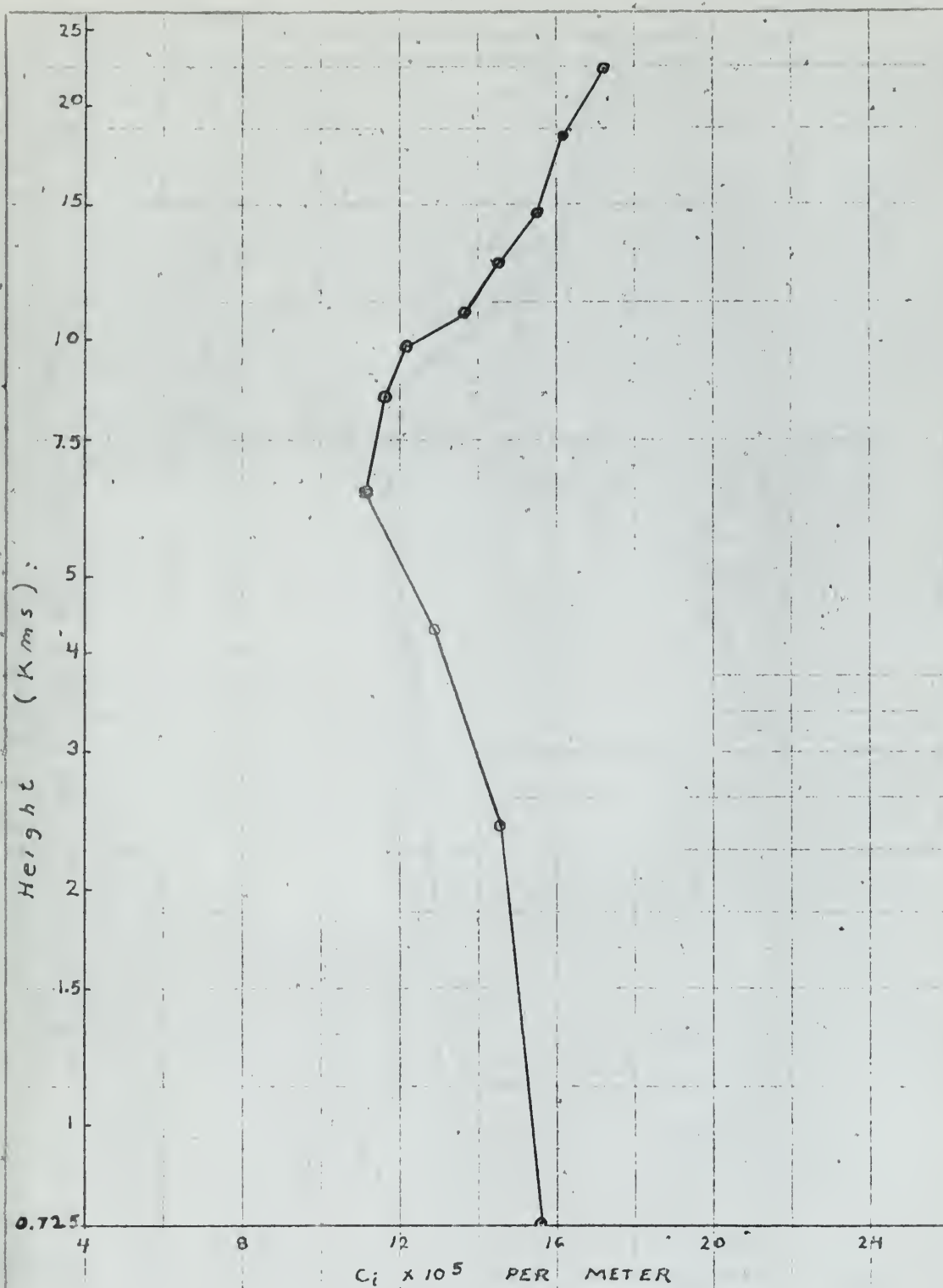


Figure 8. The graph of C_l vs height for Ship "N".

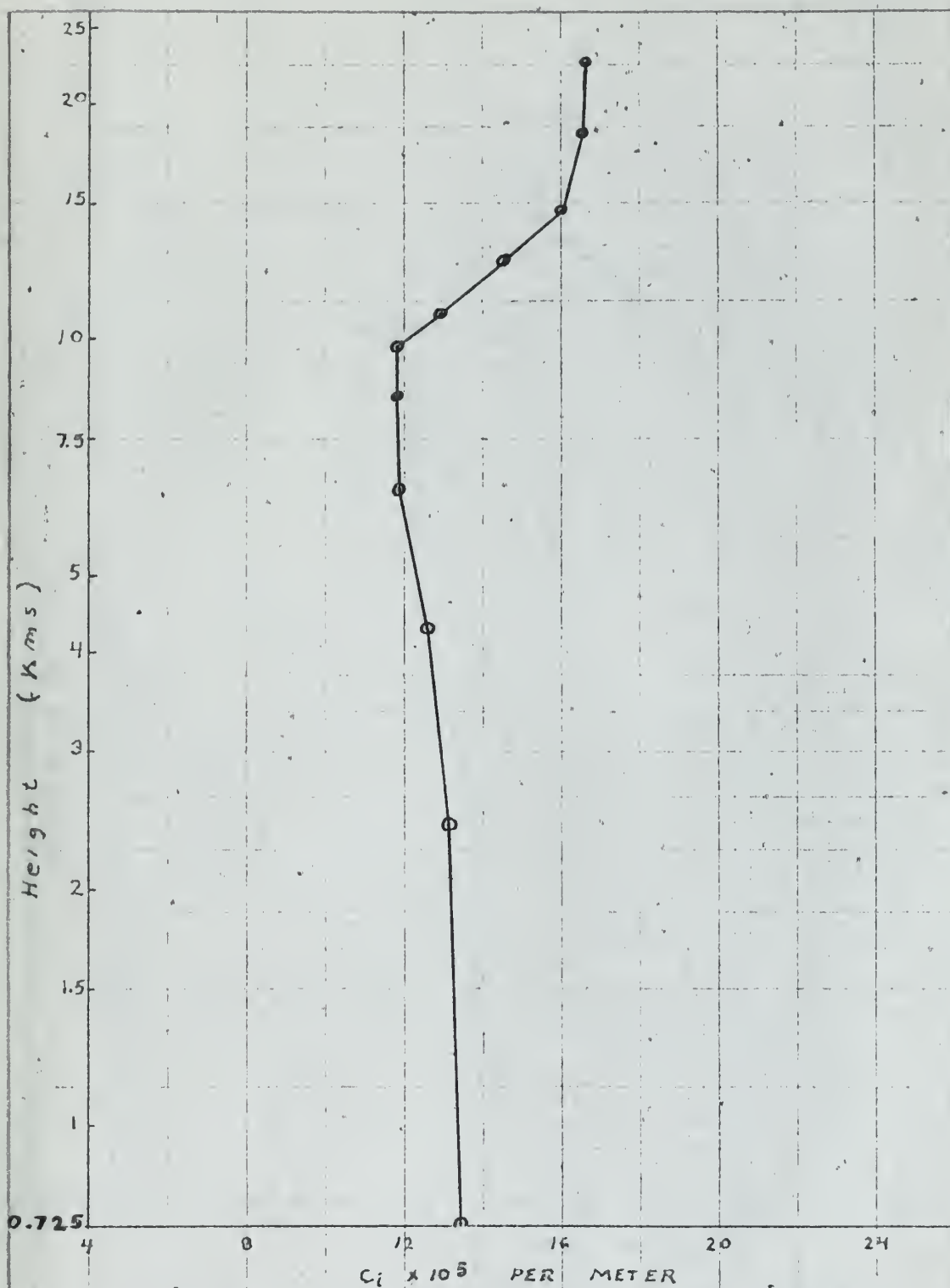


Figure 9. The graph of C_i vs height for Lake Charles.

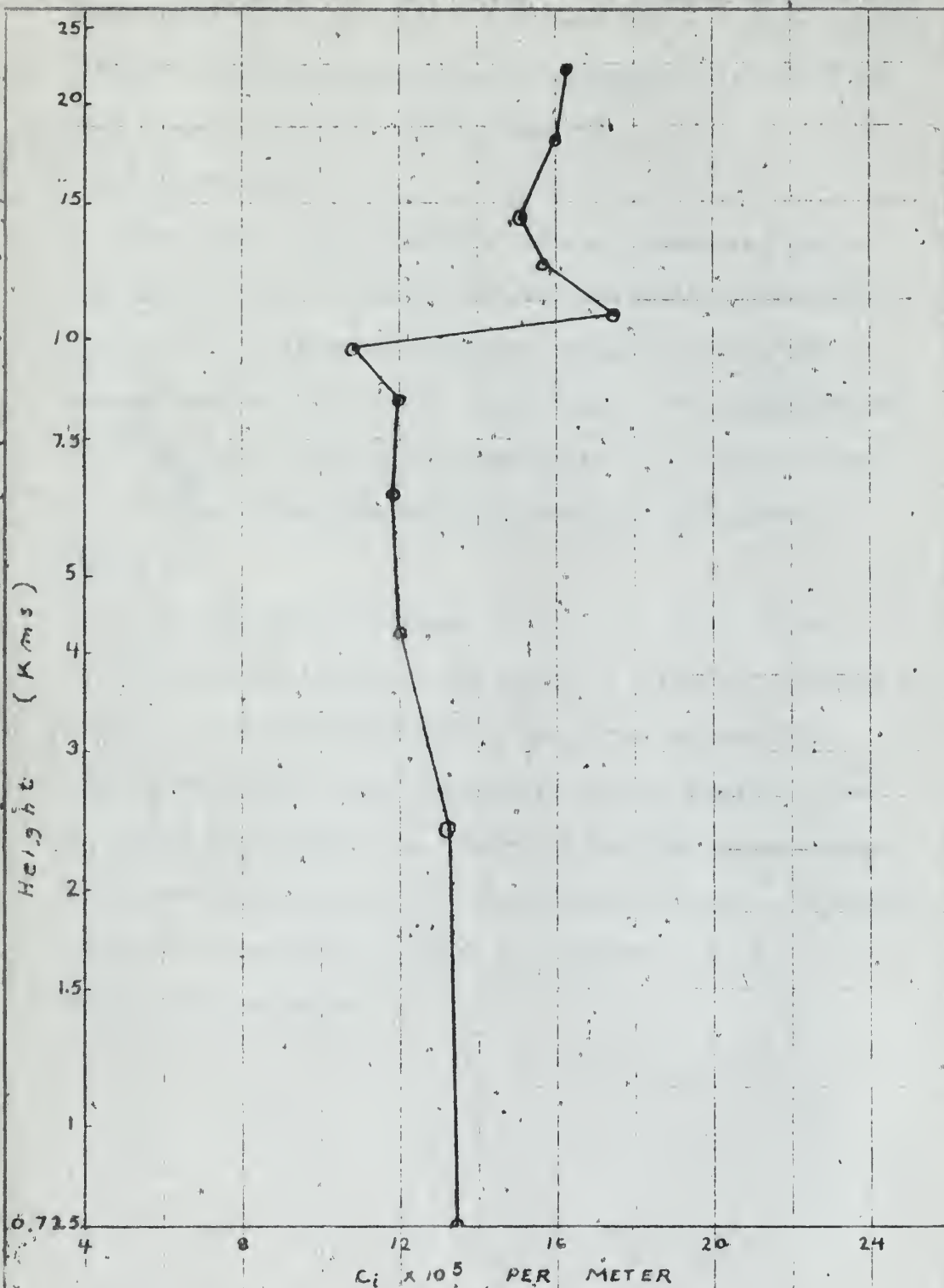


Figure 10. The graph of C_i vs height composite of all stations.

low levels at this subtropical maritime station. Thus the low-level values of c_i are larger than those for most other stations, although the minimum just below the tropopause has nearly the same value (about 11.5×10^{-5} per meter).

(f) Lake Charles

The graph for Lake Charles, Figure 9, shows the tropospheric c_i -value decreasing to a minimum which extends from 6 km to 10 km. Above this layer, c_i increases to a nearly constant maximum value in the stratosphere. The constant c_i in the range 6-10 km is a characteristic of variable tropopause height, during the observation period (c.f. Kodiak, Figure 6).

(g) Composite of all stations

The composite graph of all stations, Figure 10, conforms closely to the idealized model. The c_i -value decreases slowly with height in the troposphere, and is separated from the larger stratospheric c_i -values by the dual discontinuity. A secondary tropopause is also indicated by the less pronounced upper dual discontinuity in the neighborhood of 15 km, within the stratosphere.

4. Other Applications and Conclusions

By means of Equation (6) a method of solving for c_i between mandatory radiosonde levels was established. The resulting value of c_i was there the mean value for the layer of thickness $\Delta Z_i = Z_{i+1} - Z_i$. However c_i turns out to be somewhat variable with height. Thus in Figures 2 through 9, all graphs of c_i vs height have been drawn as continuous functions. This means that Equation (4) may be reconsidered from the viewpoint that c_i be variable with height in any layer. In this case, however, the mean value \bar{c}_i between standard levels shall be the same as that computed by Equation (6).

In the field of radar-propagation, one frequently must deal with the ray-curvature $K = d\beta/ds$ given by

$$K = 10^{-6} \left(\frac{dN}{dz} + 0.48 \right) \cos \beta \quad (9)$$

where β is the ray-direction relative to the spherically horizontal level [3]. Up to several years ago, it was customary to use as a standard dN/dz , a value characteristic of the low troposphere, namely $dN/dz = -\frac{1}{4} \left(\frac{1}{a} \right)$ where a is the radius of earth. We know now from the work of Bean and Thayer and others (including this work) that $(dN/dz)_{avg}$ is negative but decreases in magnitude. Thus, by Equation (5) with c_i and N both decreasing with height in the troposphere, $\left| dN/dz \right|$ would be relatively small just below the tropopause.

Consider still another refinement in Equation (4),

namely, that c_i is empirically given as a function of height of the type shown in Figures 2 through 9, inclusive, for the localities considered. Then logarithmic differentiation of Equation

(4) gives
$$\frac{1}{N} \frac{dN}{dz} = - \left[c_i + (z - z_i) \frac{dc_i}{dz} \right]$$

or
$$\frac{dN}{dz} = -N \left[c_i + (.4343) \frac{dc_i}{d \log_{10}(z - z_i)} \right] \quad (10)$$

This expression for dN/dz has a correction factor, as compared with Equation (5), given by the second term on the right side of (10). Actually this term can be readily computed in finite differences from graphs of c_i vs $\log_{10}(z - z_i)$ (for example, see Figures 2 through 9). The correction factor may take on some importance in radar-propagation in the tropopause layer, in view of the large increase of c_i with elevation occurring there.

Finally it should be noted that if an equation of the Bean and Thayer type, Equation (3), is desired. It may be shown that \bar{c} is a weighted-mean of the individual c_i , or

$$z_{n+1}, \bar{c} = c_n \Delta z_n + \dots + c_1 \Delta z_1 \quad (11)$$

Equation (11) makes it apparent that the use of a mean \bar{c} for the troposphere is reasonable. However, it suggests that one should use a different weighted-mean for the lower stratosphere than for the troposphere. In Equation (11), z_{n+1} is the height above the surface, so that the averaging must extend down to the earth's surface. Equation (11) may be readily solved for \bar{c} using any graph of the type shown in

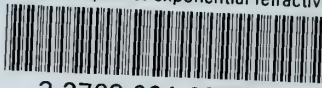
Figures 2 through 9, by selecting the c_i -values and weighting them by the indicated thicknesses ΔZ_i . However, it should be remembered that in most cases only half of the lowest layer, ΔZ_1 , is shown in these figures. For the stations studied in this paper, the N_s -values appropriate to the Bean and Thayer exponential form, Equation (3), are listed in the first row of Table 1.

BIBLIOGRAPHY

1. Bean B. R., and G. D. Thayer, Models of the atmospheric radio refractive index, Proc. I. R. E., 47, pp. 470-755. May 1959.
2. Daily series, synoptic weather maps, Part II Northern Hemisphere data tabulations, U. S. Department of Commerce.
3. Kerr, D. E., 1951. Propagation of short radio waves. McGraw-Hill Book Company, Inc., 728 pp.
4. Smith E. K., and S. Weintraub, The constants in the equation for atmospheric refractive index at radio frequencies, Proc. I. R. E., 41, pp. 1035-1037.

thesW2203

Some examples of exponential refractivit



3 2768 001 92854 2

DUDLEY KNOX LIBRARY